LASER APPLICATOINS AND OTHER TOPICS IN QUANTUM ELECTRONICS PACS numbers: 42.25.Bs; 42.81.Dp
DOI: 10.1070/QE2002v032n01ABEH002127

Time correlation analysis of the propagation of low-coherence radiation in an optical channel with imperfections of anisotropy

V.M.Gelikonov, R.V.Kuranov, A.N.Morozov

***Abstract*. The propagation of polarised low-coherent radiation is studied in an anisotropic single-mode glass fibre with imperfections of anisotropy. These imperfections are typical for interferometers used in devices for optical coherence tomography and can be caused by an inaccurate splicing of fibres or by their compression. The appearance of parasitic interference peaks due to anisotropic inhomogeneities is considered theoretically. The subtraction of parasitic peaks with orthogonal polarisations is studied theoretically and experimentally. The obtained experimental data well agree with theoretical estimates. The results of the paper are important for improving the methods for calculating interference schemes and for diagnostics of their defects.**

Keywords: *low-coherent interferometry, anisotropic optical fibres, imperfections of anisotropy, correlation time analysis, optical coherence tomography*.

1. Introduction

Great interest in interference schemes using low-coherent radiation sources has been expressed in optics, and especially in fibre optics, from the early 1980s of the 20th century. This interest is caused by the advent of comparatively low-cost, reliable, and compact sources such as superluminescent semiconductor diodes and superluminescent sources based on active fibres, which have the high spatial coherence and high spectral brightness.

These sources are mainly used in fibre gyroscopes [1 – 3] and optical coherence tomography [4 – 6]. The use of polarisation-maintaining optical fibres in low-coherent interference schemes substantionally decreases the influence of a random change of polarisation state in one of the arms of an isotropic fibre interferometer due to bends and stresses. This effect leads to the unpredictable modulation of the amplitude of an interference signal related to the intrinsic properties of the interferometer rather than to the properties of an object under study.

Despite considerable successes achieved in the above fields, these systems are still described using the methods developed by Jones as early as the 1940s of the last century (see, for example, [7 – 10]). Jones considered a change in the polarisation state during the propagation of monochromatic radiation along an anisotropic optical path. In the case of broadband radiation, the applicability of this method is limited by the lengths that do not exceed the depolarisation length L_d, i.e., a path in the optical system after the propagation of which the electric fields with orthogonal polarisations are no longer coherent. This is explained by the fact that the difference of delays acquired by radiations with different polarisations exceeds the coherence time of the source.

Later, the other authors modified the Jones method for low-coherent sources and lengths exceeding L_d [11 – 13]. The authors of papers [11 – 13] calculated the characteristics of radiation for individual monochromatic components using the Jones matrices and determined the parameters of broadband radiation by integrating over the entire wavelength range.

This method is not always convenient, in our opinion, because it lacks first of all the clarity: calculations are performed for coherent light for which the effects related to low coherence can be absent, resulting in a more higher probability of errors and a complicated interpretation of these effects. Second, it is usually impossible to perform complete analytic calculations of systems consisting of many optical elements or having optical inhomogeneities with random parameters.

Computer-aided calculations by this method are time consuming [14, 15] because the number of discrete spectral components n required for the calculation of the optical system increases proportionally to the difference of the optical paths of the eigenpolarisation axes of an anisotropic channel and inversely proportionally to the length of a coherent train: $n \sim l\Delta n_a/(c\Delta\tau_c)$, where l is the optical path; Δn_a is the difference of the refractive indices of intrinsic axes of the anisotropic optical path; $\Delta\tau_c$ the coherence time of the source; and c is the speed of light. For this reason, the papers appeared in which some simple problems of this type were qualitatively analysed using the time correlation approach [16, 17]. This makes it possible to explain simply some effects observed and perform quantitative experimental estimates.

The aim of this paper is to develop the method for describing polarised low-coherence radiation propagating along an optical path with imperfections of anisotropy, to illustrate this method for simple examples, and to verify experimentally the results of the analysis.

V.M.Gelikonov, R.V.Kuranov, A.N.Morozov Institute of Applied Physics, Russian Academy of Sciences, ul. Ul'yanova 46, GSP-120, 603950 Nizhnii Novgorod, Russia; e-mail: roman@ufp.appl.sci-nnov.ru

Received 13 August 2001
Kvantovaya Elektronika **32** (1) 59 – 65 (2002)
Translated by M.N.Sapozhnikov

2. Time correlation analysis of the propagation of light in spliced polarisation-maintaining optical fibres

The time correlation approach is based in the general case on the consideration of propagation of individual coherent pulse trains, each of these trains being a source of secondary coherent pulse trains. Let us illustrate this by the example of two spliced anisotropic fibres (Fig. 1). A Michelson interferometer is used here to estimate the quality of the mutual orientation of axes of fibres being spliced. Let the radiation from a superluminescent diode $\boldsymbol{E}(t) = \boldsymbol{E}_{\rm in}E_0(t)$ be linearly polarised at an angle of θ_1 to the intrinsic axes x', y' of the first fibre A, while the axes of the second fibre B are directed at an angle of θ_2 with respect to the axes of the first fibre. Here, $E_0(t)$ is the time dependence of the electric field strength at the input to the first fibre and $\boldsymbol{E}_{\rm in}$ is the dimensionless vector describing the polarisation state and the field amplitude $\boldsymbol{E}$ at the input of the first fibre. In this case, one coherent pulse train will propagate with delays τ_{1x} and τ_{1y} along each of the axes x' and y', respectively, at the output from the first fibre (we omit primes at subscripts x and y for brevity). The amplitudes of the trains propagating along axes x and y are $A_x = E_{\rm in}\cos\theta_1$ and $A_y = E_{\rm in}\sin\theta_1$. Because the axes of the first and second fibres do not coincide, each of the trains gives the projections both on the x and y axes, so that two pulse trains will propagate along each of the axes in the second fibre.

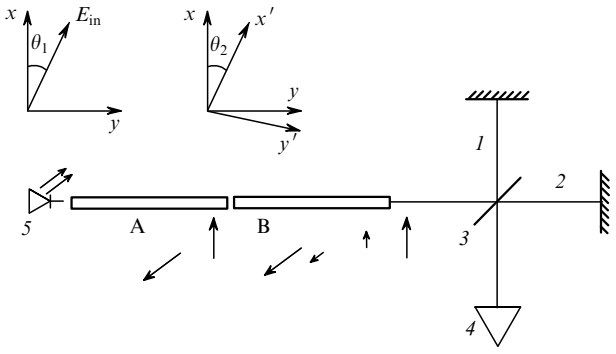

Figure 1. Illustration of the appearance of coherent trains of radiation pulses with orthogonal polarisations upon splicing of two anisotropic fibres: (*1, 2*) interferometer arms; (*3*) beamsplitter (3 dB); (*4*) photodetector; (*5*) superluminescent diode. The arrows correspond to coherent trains.

Therefore, two trains with delays $\tau_{1x}+\tau_{2x}$ and $\tau_{1y}+\tau_{2x}$ and amplitudes $B_{1x} = E_{\rm in}\cos\theta_1\cos\theta_2$ and $B_{2x} = E_{\rm in}\sin\theta_1\times\sin\theta_2$, will propagate from the second fibre along the x axis, and two trains with delays $\tau_{1y}+\tau_{2y}$ and $\tau_{1x}+\tau_{2y}$ and amplitudes $B_{1y} = E_{\rm in}\sin\theta_1\cos\theta_2$ and $B_{2y} = -E_{\rm in}\cos\theta_1\times\sin\theta_2$ will propagate along the y axis. The parameters of secondary coherent pulse trains are analysed with the Michelson interferometer, whose axes are made coincident with the axes of the second fibre. Assuming that a beamsplitter in Fig. 1 is isotropic, i.e., the power division coefficients for radiation with x and y polarisations are equal ($\kappa_x = \kappa_y = \kappa$), we write the expression for the components of the autocorrelation function along axes x y in the form

$$G_x(\tau) = 2\kappa(1-\kappa)[(\cos^2\theta_1\cos^2\theta_2 + \sin^2\theta_1\sin^2\theta_2)$$

$$\times E_{\rm in}^2 G_0(\tau) + \sin\theta_1\cos\theta_1\sin\theta_2\cos\theta_2\,E_{\rm in}^2\,G_1(\tau\pm\Delta\tau)], \quad (1)$$

$$G_y(\tau) = 2\kappa(1-\kappa)[(\sin^2\theta_1\cos^2\theta_2 + \cos^2\theta_1\sin^2\theta_2)$$

$$\times E_{\rm in}^2 G_0(\tau) - \sin\theta_1\cos\theta_1\sin\theta_2\cos\theta_2\,E_{\rm in}^2\,G_1(\tau\pm\Delta\tau)], \quad (2)$$

where $G_0(\tau) = \langle E_0(t)E_0(t+\tau)\rangle$ is the initial autocorrelation function of the source (the random process $E_0(t)$ is assumed stationary); the angle brackets denote time averaging; $G_1(\tau\pm\Delta\tau)$ is the cross-correlation function; $\Delta\tau = \tau_{1x} - \tau_{1y}$ is the difference of delays for radiations with x and y polarisations in the first fibre. The sign $\pm$ reflects the symmetry of the autocorrelation function. Physically, this means the situation when the first arm of the interferometer is shorter than the second one or when the second arm is shorter than the first one (see Fig. 1).

One can see from (1) and (2) that, in the absence of dichroism in the optical path or anisotropy of the division coefficient, for each of the trains propagating along the x axis with the nonzero delay (the condition $\tau = 0$ means the equality of the interferometer arms), a pulse train can be found that propagates along the y axis with the same delay and the amplitude that is equal in modulus but has the opposite sign. Such trains will subtract from each other upon addition [see expression (3) below]. Therefore, the total autocorrelation function will not have the term with the delay corresponding to the propagation of trains with different polarisations in the first fibre:

$$G(\tau) = G_x(\tau) + G_y(\tau) = 2\kappa(1-\kappa)E_{\rm in}^2 G_0(\tau)$$

$$= 2\kappa(1-\kappa)I_0 G_0(\tau), \quad (3)$$

where I_0 is the initial radiation intensity entering the interferometer. This means that, in the absence of dichroism or anisotropy of the division coefficient, we cannot determine the mutual orientation of the spliced fibres. In the presence of anisotropy of the division coefficient in the interferometer ($\kappa_x \neq \kappa_y$), the subtraction of the trains mentioned above will be incomplete. The subtraction depth is defined by the coefficient

$$\eta = \frac{\left|[\kappa_x(1-\kappa_x)]^{1/2} - [\kappa_y(1-\kappa_y)]^{1/2}\right|}{\left|[\kappa_x(1-\kappa_x)]^{1/2} + [\kappa_y(1-\kappa_y)]^{1/2}\right|}, \quad (4)$$

where $\eta = 0$ means the complete subtraction and $\eta = 1$ corresponds to the absence of subtraction.

Let us assume that the length of the first fibre is longer than the depolarisation length $L_{\rm d} = \lambda_0^2/(\Delta\lambda\Delta n_{\rm a})$, where λ is the central wavelength of the source in vacuum; $\Delta\lambda$ is the characteristic spectral width of the emission band of the source. This corresponds to the situation when the interference pattern will exhibit, in the presence of dichroism or anisotropy of the division coefficient, a separate interference region (hereafter, the correlation or interference peak) with the delay $\Delta\tau$ because the two trains propagating with different initial polarisations and the same delay will be separated after some time by the length exceeding the correlation length. For a source with the emission spectrum of width 20 nm, the central wavelength of 0.8 μm, and the

birefringent refractive index $\Delta n_a = 1.5 \times 10^{-4}$, the depolarisation length is 21 cm.

Therefore, a separate correlation peak corresponding to the splicing region of two fibres can be observed already in a short piece of an anisotropic fibre. One can see from (1) and (2) that the best conditions for the observation of this peak (when the peak amplitude is maximal for the given θ_2) are obtained when the polarisation modes of the first fibre are excited with the same rate, and radiation with one of the polarisations does not fall on a photodetector. In this case, the subtraction is completely absent.

The wave with one of the polarisations can be suppressed by placing a polariser between the second fibre and a photodetector, whose axis is made coincident with one of the axes of the second fibre. The amplitude of the correlation peak changes depending on the angle between the axes of spliced fibres from zero (when the axes coincide or orthogonal) to the maximum equal to 0.5 of the main peak amplitude (when the angle between the axes of the fibres is 45°). The correlation-peak amplitude changes from the maximum (when the axes are coincide or orthogonal) to zero (for 45°) depending on the angle between the transmission axis of the polariser and the axes of the output fibre.

The appearance of new components of the field with the given polarisation from the components with the orthogonal polarisation (energy transfer) upon splicing two anisotropic fibres can be described with a matrix of rotation by the mismatch angle θ_2 of the intrinsic axes of spliced fibres

$$O(\theta_2) = \begin{pmatrix} \cos\theta_2 & \sin\theta_2 \\ -\sin\theta_2 & \cos\theta_2 \end{pmatrix}. \tag{5}$$

In this case, the fields along the axes x and y at the output of the second fibre can be written in the form

$$\begin{aligned} E_x &= E_{in}[E_1(t+\tau_{1x})\cos\theta_1\cos\theta_2 \\ &\quad + E_2(t+\tau_{1y})\sin\theta_1\sin\theta_2], \\ E_y &= E_{in}[-E_1(t+\tau_{1x})\cos\theta_1\sin\theta_2 \\ &\quad + E_2(t+\tau_{1y})\sin\theta_1\cos\theta_2]. \end{aligned} \tag{6}$$

Such a representation of the output-field components is convenient for analysis of more complicated systems, for example, in the case of distributed inhomogeneities, multiple imperfections of anisotropy, etc.

3. Time correlation analysis in the case of an artificially induced imperfections of anisotropy in a polarisation-maintaining optical fibre

The radiation energy transfer from one polarisation to another can occur in anisotropic fibres not only upon their splicing but also due to intrinsic or induced inhomogeneities in the fibre. We will consider here only the induced inhomogeneities, assuming the imperfections of anisotropy appearing upon fibre manufacturing to be small. Consider the case that is analogous to that described above (Fig. 1), but in the absence of the second fibre B. We assume that the intrinsic axes of the first fibre A coincide with the axes of the interferometer.

Let the first anisotropic fibre be subjected to a force directed orthogonal to the propagation direction of radiation, and this direction does not coincide in the general case with the direction of the eigenpolarisation axes x or y of the fibre ($\alpha \neq 0$ in Fig. 2a). As shown in paper [18] for an isotropic fibre, energy transfer occurs most efficiently if the force acts in one direction. The force can appear due to the fibre compression or, for example, due to the nonuniform action of the glue fastening the fibre to a piezoceramic plate modulating the optical path in the interferometer arms [19–21]. We assume that only radiation with a simplest transverse structure HE_{11} can propagate in each of the two polarisation modes.

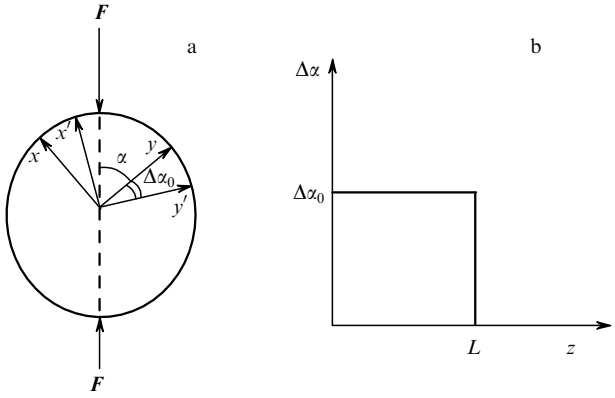

Figure 2. Orientation of the initial polarisation axes and axes induced by the force ***F*** directed at an angle of α to the eigenpolarisation axes of an anisotropic fibre and perpendicular to the z axis of radiation propagation (a), and the dependence of the angle $\Delta\alpha$ between the induced and eigenpolarisation axes of the anisotropic fibre on z (b).

We assume that the action length along the z axis is $L \ll L_d$, the action experiencing a discontinuity depending on z. In the region of the force action, new intrinsic axes x', y' of the modified fibre appear (Fig. 2a), which are directed with respect to the axes x, y of the unmodified fibre at an angle $\Delta\alpha$, which depends on the force amplitude and direction. The dependence of $\Delta\alpha$ on z in this case is show in Fig. 2b. Then, the time dependence of the polarisation components of the electric field immediately after the induced inhomogeneity can be represented in the form

$$\begin{aligned} E_x(t) &= E_{in}\left[\cos\theta_1 \int u_{11}(\omega)E(\omega)e^{i\varphi_{1x}(\omega)}e^{i\omega t}d\omega \right. \\ &\quad \left. + \sin\theta_1 \int u_{12}(\omega)E(\omega)e^{i\varphi_{1y}(\omega)}e^{i\omega t}d\omega\right], \\ E_y(t) &= E_{in}\left[\cos\theta_1 \int u_{21}(\omega)E(\omega)e^{i\varphi_{1x}(\omega)}e^{i\omega t}d\omega \right. \\ &\quad \left. + \sin\theta_1 \int u_{22}(\omega)E(\omega)e^{i\varphi_{1y}(\omega)}e^{i\omega t}d\omega\right], \end{aligned} \tag{7}$$

where ω is the circular frequency; $E(\omega) = \int E_0(t)e^{-i\omega t}dt$ is the Fourier component of the function $E_0(t)$; $u_{jh}(\omega)$ are the components of the Jones matrix $\hat{U}(\omega)$ for the given frequency ω; $\varphi_{1x.1y}(\omega)$ are the phase incursions along axes x and y of the first fibre until the induced inhomogeneity. The Jones matrix $\hat{U}(\omega)$ in this case is determined as a product of three matrices

$$\hat{U}(\omega) = \mathrm{e}^{i\xi} O(-\Delta\alpha_0)\Phi(\rho(\omega))O(\Delta\alpha_0) = \tag{8}$$

$$\begin{pmatrix} \mathrm{e}^{\mathrm{i}\rho(\omega)}\cos^2\Delta\alpha_0 + \mathrm{e}^{-\mathrm{i}\rho(\omega)}\sin^2\Delta\alpha_0 & -\mathrm{i}\sin(2\Delta\alpha_0)\sin\rho(\omega) \\ -\mathrm{i}\sin(2\Delta\alpha_0)\sin\rho(\omega) & \mathrm{e}^{-\mathrm{i}\rho(\omega)}\cos^2\Delta\alpha_0 + \mathrm{e}^{\mathrm{i}\rho(\omega)}\sin^2\Delta\alpha_0 \end{pmatrix}$$

where

$$\Phi(\rho(\omega)) = \begin{pmatrix} \mathrm{e}^{\mathrm{i}\rho(\omega)} & 0 \\ 0 & \mathrm{e}^{-\mathrm{i}\rho(\omega)} \end{pmatrix}; \quad \xi = 0.5(\beta_x + \beta_y)L;$$

$$\rho(\omega) = 0.5\Delta\beta(\omega)L; \quad \Delta\beta(\omega) = \beta_x(\omega) - \beta_y(\omega);$$

$\beta_{x,y}$ are the propagation constants of waves with polarisations along axes x and y, respectively.

The above expressions neglect changes in the propagation constants caused by the action on the fibre because an external force was assumed small compared to stresses inside the fibre that are required for producing high birefringence. To take this effect into account, we should add to $\Delta\beta$ the term $\Delta\beta_{\mathrm{ind}}$ caused by the external force ($\Delta\beta_{\mathrm{ind}} \ll \Delta\beta$). Below, we will omit the common phase factor ξ because only the phase difference is important in interference schemes.

The frequency dependence of the elements of the Jones matrix can be neglected if the characteristic scale of their variation is much larger than the characteristic scale of variation $\Delta\omega$ of the power spectrum $S(\omega) = \langle |E(\omega)|^2 \rangle$ of the source. One can see from (8) that this condition gives

$$\frac{2\mathrm{d}\rho}{\mathrm{d}\omega}\Delta\omega = \frac{\mathrm{d}\Delta\beta}{\mathrm{d}\omega}\Delta\omega L \ll 2\pi. \tag{9}$$

Taking into account that $\Delta\omega = (2\pi c/\lambda_0^2)\Delta\lambda$, $\Delta\beta(\omega) = k(\omega)\Delta n_{\mathrm{a}}$, where $k(\omega) = \omega/c$ is the wave number, and c is the speed of light in vacuum, we obtain from (9)

$$\frac{L}{L_{\mathrm{d}}} \ll 1, \text{ or } L \ll L_{\mathrm{d}}. \tag{10}$$

Therefore, when the action length along the z axis is much shorter than the depolarisation length, expression (7) can be written in the form

$$\begin{aligned} E_x(t) &= E_{\mathrm{in}}[\cos\theta_1 u_{11}(\omega_0)E(t+\tau_{1x}) \\ &\quad + \sin\theta_1 u_{12}(\omega_0)E(t+\tau_{1y})], \\ E_y(t) &= E_{\mathrm{in}}[\cos\theta_1 u_{21}(\omega_0)E(t+\tau_{1x}) \\ &\quad + \sin\theta_1 u_{22}(\omega_0)E(t+\tau_{1y})], \end{aligned} \tag{11}$$

where $\omega_0 = 2\pi c/\lambda_0$ is the central frequency of the source.

Below, we will write u_{jh} instead of $u_{jh}(\omega_0)$. One can see from (8) that the radiation power transferred from one polarisation to another (nondiagonal elements of the matrix $\hat{U}(\omega)$) depends not only on the rotation of the axes induced by the external force but also on the difference in the phase incursion for radiations with two orthogonal polarisations in the interaction region. When the action length equals to an integer of the beat wavelengths in the given fibre, no energy transfer occurs between polarisation modes.

In reality, a force cannot appear abruptly, and the fibre axes do not undergo a discontinuity. In the case of an arbitrary continuous coordinate dependence of the angle z $\Delta\alpha = \Delta\alpha(z)$ induced by the force $\boldsymbol{F}(z)$, this dependence can be approximated by a set of dependences in the form of steps of length Δz and then direct Δz to zero. After the passage to the limit, the exclusion of the dependence on the common phase factor $\mathrm{e}^{\mathrm{i}\xi}$ and the change of variables $E_{1x} = E_x\mathrm{e}^{\mathrm{i}\xi}$ and $E_{1y} = E_y\mathrm{e}^{\mathrm{i}\xi}$, we obtain the system of differential equations for the electric-field components

$$\begin{aligned} \frac{\mathrm{d}E_{1x}}{\mathrm{d}z} &= E_{1y}\frac{\mathrm{d}\Delta\alpha}{\mathrm{d}z} + \frac{1}{2}\mathrm{i}\Delta\beta E_{1x}, \\ \frac{\mathrm{d}E_{1y}}{\mathrm{d}z} &= -E_{1x}\frac{\mathrm{d}\Delta\alpha}{\mathrm{d}z} - \frac{1}{2}\mathrm{i}\Delta\beta E_{1y}. \end{aligned} \tag{12}$$

For the given dependence $\Delta\alpha = \Delta\alpha(z)$, this equation can be solved numerically. Fig. 3 shows the dependences of the relative amplitude of the transferred field component

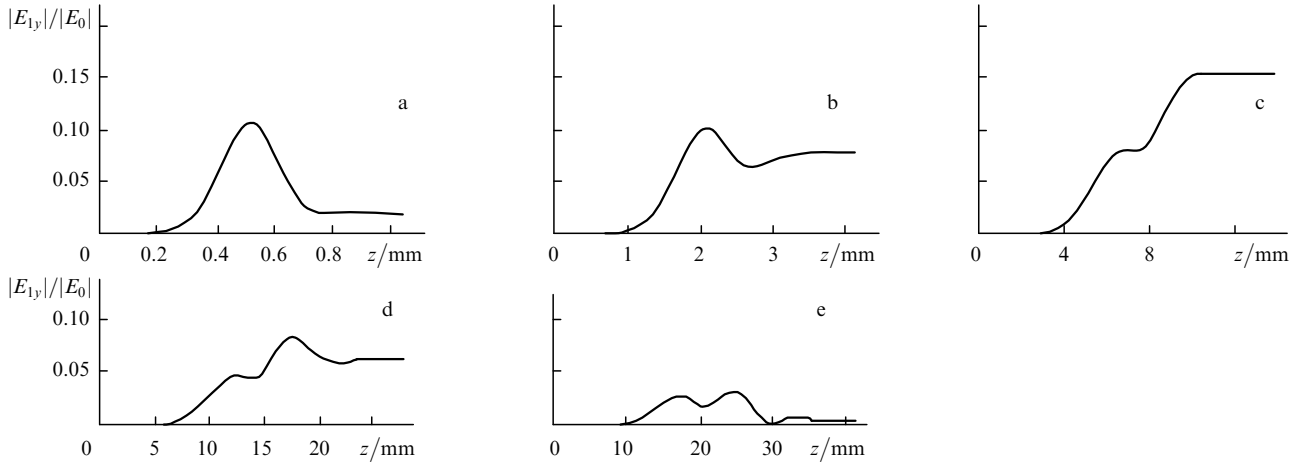

Figure 3. Results of he numerical solution of equation (12) for $\Delta\alpha(z) = \Delta\alpha_0 \exp[-(z-z_0)^2/2L_{\mathrm{i}}^2], z_0 = 5L_{\mathrm{i}}, E_{1x}(0) = E_0, E_{1y}(0) = 0, \Delta n_{\mathrm{a}} = 1.5 \times 10^{-4}$,, $\lambda = 0.83$ μm, $\Delta\alpha_0 = \pi/30$ and $\Delta\beta L_{\mathrm{i}} = \pi/40$ (a), $\pi/10$ (b), $\pi/3$ (c), $\pi/1.5$ (d), and π (e).

$|E_{1y}|/|E_0|$ on z, which were obtained by the numerical simulation of equations (12), where $|E_0|$ is the amplitude of the input field component $E_{1x}(0)$ ($E_{1y}(0) = 0$), by varying the induced rotation angle according to the Gaussian law.

When the length of the induced inhomogeneity is small ($\Delta\beta L_i \ll 1$), the power transfer from one polarisation mode to another is very weak because almost all the power transferred at the positive derivative $d\Delta\alpha(z)/dz$ of the induced rotation angle is transferred back at the negative derivative due to the absence of the incursion of the phase difference in polarisation modes (Fig. 3a). When the inhomogeneity length increases, the amplitude of the transferred component first increases proportionally to the phase difference incursion $\Delta\varphi_i = \Delta\beta L_i$ (Fig. 3b), achieves the maximum (Fig. 3c), and then tends to zero with increasing L_i (Figs. 3d, e).

The transferred power reaches the maximum when, in the case of the negative derivative of the rotation angle, the polarisation components are out of phase. In this case, the terms $E_{1y}d\Delta\alpha/dz$ and $E_{1x}d\Delta\alpha/dz$ in equation (12) are always positive, i.e., the power is transferred only from one polarisation mode to another, for example, from radiation polarised along the x axis to radiation polarised along the y axis, both in the cases of the positive and negative derivatives of the induced rotation angle. As the length of the induced inhomogeneity further increases, these terms become alternating, so that the power is transferred alternatively between the polarisation modes. In addition, the amplitude of the transferred component becomes limited because of a weak coupling between the modes, because in this case ($d\Delta\alpha(z)/dz \ll \Delta\beta$) the maximum possible transferred power is $P_{max} \sim \Delta\alpha_0^2(L_i\Delta\beta)^{-2}$ [22].

It has been shown in papers [7, 8] that the propagation of coherent radiation in any anisotropic optical system without dichroism can be described by a product of unitary matrices. The production of any number of unitary matrices is also a unitary matrix [8]. Therefore, each matrix describing the appearance of new field components with a given polarisation from the electric field with the orthogonal polarisation is unitary. The unitary matrix can be written in the general form as

$$\hat{U} = \begin{pmatrix} e^{i\phi}\cos\theta & -e^{-i\psi}\sin\theta \\ e^{i\psi}\sin\theta & e^{-i\phi}\cos\theta \end{pmatrix}. \qquad (13)$$

All the parameters in (13) are real. For example, by comparing (13) with (8), we can write

$$\cos\theta = [1 - \sin^2\rho\sin^2(2\Delta\alpha_0)]^{1/2},\ \sin\theta = \sin\rho\sin(2\Delta\alpha_0),$$
$$\psi = \pi/2,\ \phi = \tan\rho\cos(2\Delta\alpha_0). \qquad (14)$$

By using (11) and (13), we write the expression for the interference signal in the case of an induced inhomogeneity in the form

$$G_x(\tau) = 2\kappa(1-\kappa)[(\cos^2\theta_1\cos^2\theta + \sin^2\theta_1\sin^2\theta)E_{in}^2G_0(\tau)$$
$$- \sin\theta_1\cos\theta_1\sin\theta\cos\theta\,E_{in}^2\,G_1(\tau\pm\Delta\tau)e^{i(\phi+\psi)}], \qquad (15)$$

$$G_y(\tau) = 2\kappa(1-\kappa)[(\sin^2\theta_1\cos^2\theta + \cos^2\theta_1\sin^2\theta)E_{in}^2G_0(\tau)$$
$$+ \sin\theta_1\cos\theta_1\sin\theta\cos\theta\,E_{in}^2\,G_1(\tau\pm\Delta\tau)e^{i(\phi+\psi)}]. \qquad (16)$$

The total interference signal is described by expression (3), as in the first case of splicing two fibres. When the losses in waves with orthogonal polarisations are the same, a common factor will appear in front of the matrix in (13) [9], which only reduced the amplitude of the total interference signal as a whole. This factor has no effect on all other conclusions, so that all the results remain valid for systems without dichroism and anisotropy of the division coefficient.

4. Experimental study of subtraction of interference peaks

Fig. 4 shows the scheme of the experimental setup for the observation and study of the subtraction of interference peaks. Radiation from a low-coherence source is coupled into an isotropic fibre, in which a certain polarisation state is produced with the help of a Lefevre polarisation controller [23]. Then, polarisation modes are excited with the required rate in an anisotropic fibre by light using lenses and a polariser [polariser (*5*) can be present or absent]. The artificially induced power transfer from one polarisation mode to another in the anisotropic fibre can be performed by the local action (compression in one direction) orthogonal to the direction of light propagation. The action region was about 3 mm for the depolarisation length of the anisotropic fibre equal to 21 cm. The distance from the beginning of the anisotropic fibre to the region of action was about 1 m, which is substantially greater that the depolarisation length. The induced coherent trains were observed as individual interference peaks located symmetrically on the sides of the main peak (Fig. 5) at a distance of 150 μm.

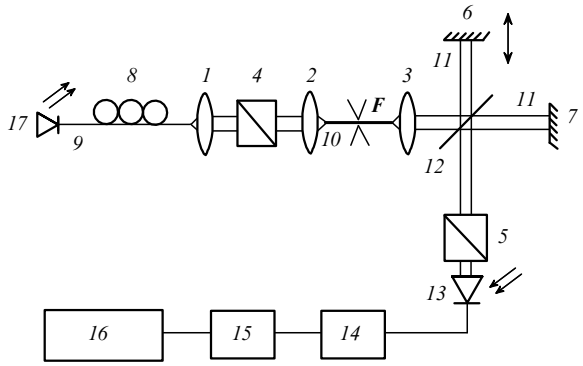

Figure 4. Scheme of the experimental setup for measuring the subtraction of the polarisation components of a low-coherence interference signal: (*1–3*) lenses; (*4, 5*) polarisers; (*6, 7*) highly reflecting mirrors; (*8*) polarisation Lefevre controller; (*9*) isotropic fibre; (*10*) anisotropic fibre (***F*** is the local force acting on the fibre); (*11*) first and second arms of the interferometer; (*12*) beamsplitter (3 dB); (*13*) photodetector; (*14*) selective amplifier; (*15*) ADC; (*16*) computer; (*17*) superluminescent diode.

A lens (*3*) (Fig. 4) forms a plane-parallel beam, which is directed to the Michelson interferometer. The path difference in the interferometer is linearly modulated by 0.5 mm with the velocity v by the periodic motion of a mirror (*6*). The interference signal is formed by a photodetector and is fed, via a selective amplifier tuned to the Doppler frequency $f_D = 2v/\lambda_0$ and an ADC, to a computer ($\lambda_0 = 0.83$ μm is the central wavelength of the source). The Doppler frequency in our experiments was 2 kHz. The polarisation state at the

interferometer output is analysed with a rotating polaroid plate with an opaque radial strip for determining the zero signal [24]. Polarisation modes are excited in the anisotropic fibre with the same rate with the help of the polarisation controller and polariser (*4*).

The experiment consisted of two parts. In the first case, polariser (*5*) was absent (Fig. 4), while in the second case, its axis was made coincident with one of the axes of the correlator. The results of measurements are shown in Fig. 5. Fig. 5a shows the dependence of the interference signal on the optical path difference in the interferometer arms in the absence of a polariser. Fig. 5b shows this dependence obtained when the axis of polariser (*5*) was made coincident with one of the axes of a low-coherent Michelson interferometer with lumped optical elements (correlator). A comparison of these dependences shows that the amplitude of the secondary correlation peak, which is caused by the external action on the fibre and by the recession of the polarisation modes on the fibre length up to region of the local action, is smaller by a factor of 5.8 in the first case (Fig. 5a) than the secondary-peak amplitude in the second case (Fig. 5b).

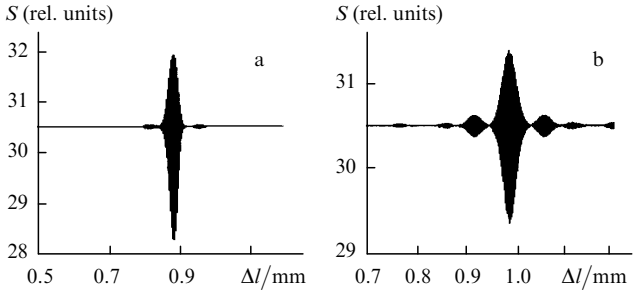

Figure 5. Dependences of the interference signal S on the optical path difference Δl in the arms of the Michelson interferometer in the absence of a polariser (a) and in the presence of polariser (*5*) (Fig. 4) whose axis coincides with one of the correlator axes.

The fact that the secondary peaks in the first case are not subtracted to zero is explained by the anisotropy of the division coefficient of the beamsplitter (Fig. 4). This can be determined in the following way. When one of the arms of the correlator is blocked, the ratio of the output radiation intensity of the correlator to its input intensity I_0 is $I_{1p} = 0.14$ for p-polarisation (with respect to the beamsplitter) and $I_{1s} = 0.108$ for s-polarisation. When another arm is blocked, the normalised output radiation intensity is $I_{2p} = 0.176$ for p-polarisation and $I_{2s} = 0.114$ for s-polarisation.

Let us assume that the amplitude of the main interference peak is greater than that of the induced peak by a factor of w, both for s- and p-polarisation, i.e.,

$$\begin{aligned} \Gamma_{mp} &= 2w_0 w (I_{1p} I_{2p})^{1/2}, \quad \Gamma_{ip} = 2w_0 (I_{1p} I_{2p})^{1/2}, \\ \Gamma_{ms} &= 2w_0 w (I_{1s} I_{2s})^{1/2}, \quad \Gamma_{is} = 2w_0 (I_{1s} I_{2s})^{1/2}, \end{aligned} \tag{17}$$

where w_0 is the common normalisation factor.

Then, in the absence of a polariser, the ratio of the intensities of the main and induced peaks is

$$\eta_+ = \frac{\Gamma_{mp} + \Gamma_{ms}}{|\Gamma_{ip} - \Gamma_{is}|} = \frac{w\left[(I_{1s} I_{2s})^{1/2} + (I_{1p} I_{2p})^{1/2}\right]}{\left|(I_{1s} I_{2s})^{1/2} - (I_{1p} I_{2p})^{1/2}\right|}. \tag{18}$$

When the axis of polariser (*5*) (Fig. 4) coincides with one of the axes of the correlator, we have

$$\eta_- = \frac{\Gamma_{mp}}{\Gamma_{ip}} = \frac{\Gamma_{ms}}{\Gamma_{is}} = w. \tag{19}$$

In this case, the subtraction coefficient is obviously defined as

$$\eta = \frac{\eta_-}{\eta_+} = \frac{\left|(I_{1s} I_{2s})^{1/2} - (I_{1p} I_{2p})^{1/2}\right|}{(I_{1s} I_{2s})^{1/2} + (I_{1p} I_{2p})^{1/2}}. \tag{20}$$

By substituting the experimental values into (20), we find $1/\eta = 5.8$, in accordance with the experimental value.

5. Conclusions

We have considered the features of the correlation time analysis of the low-coherence radiation propagated along an optical path having imperfections of anisotropy by the example of one imperfection. As such an imperfection, we considered optical inhomogeneities produced upon splicing two polarisation-maintaining optical fibres, as well as under the action of a force on a birefringent fibre perpendicular to the propagation direction of radiation. We have shown theoretically and experimentally the existence of subtraction of the coherence regions in the interference signal, which are related to imperfections of anisotropy in the optical path. We have also shown that an incomplete subtraction can occur, which is determined either by dichroism in the optical path or the anisotropy of the division coefficient of a beamsplitter used in the correlator. We have measured the subtraction efficiency caused by the anisotropy of the division coefficient of the correlator. The estimated subtraction efficiency coincides with the experimental value.

Acknowledgements. The authors thank I.A.Andronova for discussion and useful advice. This work was supported by the Russian Foundation for Basic Research (Grants Nos 99-02-16256 and 00-15-96372).

References

1. Bohm K., Marten P., Petermann K., Weidel E. *Electron. Lett.*, **17**, 352 (1981).
2. Burns W.K., Moeller R.P., Villarruel C.A., Abebe M. *Opt. Lett.*, **9**, 540 (1984).
3. Lefevre H. *The fiber-optic gyroscope* (Boston, London, Artech House, 1993) p.313.
4. Huang D., Wang J., Lin C.P., Shuman J.S., Stinson W.G., Chang W., Hee M.R., Flotte T., Gregory K., Puliafito C.A., Fujimoto J.G. *Science*, **254**, 1178 (1991).
5. Sergeev A., Gelikonov V., Gelikonov G., Feldchtain F., Pravdenko K., Shabanov D., Gladkova N., Pochinko V., Zhegalov V., Dmitriev G., Vazina I., Petrova G., Nikulin N. *Proc. SPIE, Int. Soc. Opt. Eng.*, **2328**, 144 (1994).
6. Gelikonov V.M., Gelikonov G.V., Gladkova N.D., Kuranov R.V., Nikulin N.K., Petrova G.A., Pochinko V.V., Pravdenko K.I., Sergeev A.M., Feldchtain F.I., Khanin Ya.I., Shabanov D.V. *Pis'ma Zh. Eksp. Teor. Fiz.*, **61**, 149 (1995) [*JETP Lett.*, **61**, 158 (1995)].
7. Jones R.C. *J. Opt. Soc. Am.*, **31**, 488 (1941).
8. Hurwitz H., Jones R.C. *J. Opt. Soc. Am.*, **31**, 493 (1941).
9. Poole C.D. *Opt. Lett.*, **13**, 687 (1988).
10. Smith A.M. *Appl. Opt.*, **17**, 52 (1978).
11. Kozel S.M., Listvin V.N., Shatalin S.V., Yushkaitis R.V. *Opt. Spektrosk.*, **60**, 1295 (1986).
12. Zalogin A.N., Kozel S.M., Listvin V.N. *Izv. Vyssh. Uchebn. Zaved. Ser. Radiofiz.*, **29**, 243 (1986).

13. Sakai J. *J. Opt. Soc. Am. A,* **1**, 1007 (1984).
14. Malykin G.B., Pozdnyakova V.I., Shereshevskii I.A. *Opt. Spektrosk.*, **83**, 843 (1997).
15. Malykin G.B., Pozdnyakova V.I. *Opt. Spektrosk.*, **84**, 145 (1998) [*Opt. Spectrosc.*, **84**, 131 (1998)].
16. Takada K., Chida K., Noda J. *Appl. Opt.*, **26**, 2979 (1987).
17. Mochizuki K. *Appl. Opt.*, **23**, 3284 (1984).
18. Namihira Y., Kudo M., Mushiake Y. *Electron. Commun. Jap.*, **60c** (7), 107 (1977).
19. Gelikonov V.M., Gelikonov G.V., Gladkova N.D., Leonov V.I., Sergeev A.M., Feldchtain F.I. RF Patent № 2100787 (1997).
20. Gelikonov V.M., Gelikonov G.V., Gladkova N.D., Leonov V.I., Sergeev A.M., Feldchtain F.I., Khanin Y.I. US Patent № 5867268 (1999).
21. Gelikonov V.M., Gelikonov G.V., Gladkova N.D., Leonov V.I., Sergeev A.M., Feldchtain F.I., Khanin Y.I. US Patent № 5835642 (1998).
22. Unger H.-G. *Planar Optical Waveguides and Fibres* (Oxford: Clarendon Press, 1977; Moscow: Mir, 1980).
23. Lefevre Y.C. *Electron.Lett.*, **16**, 778 (1980).
24. Malykin G.B., Stepanov D.P. *Izv. Vyssh. Uchebn. Zaved. Ser. Radiofiz.*, **33**, 255 (1990).